Cholesterol dynamics are essential for the growth and development of *Plasmodium falciparum* within the erythrocyte

Avantika I. Ahiya[a], Suyash Bhatnagar[a], Joanne Morrisey[a], Josh R. Beck[b], Akhil B. Vaidya[a*]

a. *Center for Molecular Parasitology, Institute of Molecular Medicine and Infectious Disease, Department of Microbiology and Immunology, Drexel University College of Medicine, Philadelphia, Pennsylvania 19129*

b. *Department of Biomedical Sciences, Iowa State University, Ames, Iowa 50011*

*To whom correspondence should be addressed at Center for Molecular Parasitology, Dept. of Microbiology and Immunology, Drexel University College of Medicine, 2900 Queen Lane, Philadelphia, PA 19129. Tel.: 215-991- 8557; Fax: 215-848-2271;

E-mail: av27@drexel.edu

Abstract:

Plasmodium spp. lack *de novo* cholesterol synthetic pathways and can only scavenge it from their host erythrocyte. Here we report that depletion of cholesterol from the erythrocyte plasma membrane by methyl-β-cyclodextrin (MBCD) has dramatic consequences. The removal of cholesterol results in invasion defects as well as inhibition of parasite development through the intra-erythrocytic cycle. These defects could be rescued by reconstitution with cholesterol and desmosterol but not with epicholesterol. By using live microscopy of fluorescently tagged trophozoite stage parasites, we detected rapid expulsion of the parasites from erythrocyte when exposed to MBCD for just 30 mins. Strikingly, the parasites transition from being intra-erythrocytic to extracellular within 10 seconds and do so without rupturing the erythrocyte membrane. These extruded parasites were still surrounded by the parasitophorous vacuolar membrane (PVM) and remained tethered to the erythrocyte. Electron microscopy revealed that although extracellular parasites retained their PVM, it was heavily compromised. Treatment with antimalarials that disrupt cholesterol homeostasis prior to MBCD exposure prevented the extrusion of trophozoites. These results reveal importance of cholesterol during the intra-erythrocytic development of *P. falciparum* and the dramatic consequences resulting from tampering with cholesterol content in the infected erythrocyte. These findings suggest dynamic nature of cholesterol within the infected erythrocyte that is critical for parasite survival.

Keywords:

Parasite extrusion, cholesterol dynamics, PfATP4 and PfNCR1 inhibitors, vomocytosis

Introduction:

P. falciparum, the causative agent of malaria claims around 400,000 lives yearly [1]. Due to ineffective vector control and limited availability of a potent vaccine against malaria, antimalarials are the mainstay for control and prevention of the disease. Recent work in identifying potential antimalarials has strengthened the drug development pipeline, yet drug resistance is a major hinderance in eliminating malaria. Thus, there is a constant need for developing newer antimalarials. Understanding the mechanisms of action of antimalarials under development provides insights into parasite biology which in turn can aid in identifying novel drug targets and pathways.

A salient feature of malaria parasites is their dependence on the host to fulfil their nutrient requirements. In addition to various nutrients, *Plasmodium* salvages lipids and fatty acids from the host. While the parasite possesses pathways for synthesizing and modifying lipids [2, 3], it lacks the machinery for *de novo* cholesterol synthesis [4-7]. Unlike the intrahepatic stages where the parasites have access to copious amounts of cholesterol [8], blood stage parasites can only access cholesterol present in the erythrocyte [9]. Erythrocyte also do not have the ability to synthesize cholesterol and thus depend on the amount that they were endowed with during their maturation. Investigations have revealed that intra-erythrocytic *P. falciparum* growth requires supply of fatty acids that cannot be substituted with lipids and cholesterol from serum derived lipoproteins [10]. Thus, the entire erythrocytic development of *P. falciparum* relies on the cholesterol already present within the host membrane and fatty acids from the environment. Following the invasion by merozoites, the parasite is surrounded by a parasitophorous vacuolar membrane (PVM), which is initially derived from invagination of the erythrocyte membrane [11] that expands as the parasite grows. Fluorescence lifetime imaging microscopy of *P. falciparum*-infected erythrocytes [12] indicated a downward cholesterol gradient with the maximum amount present in the erythrocyte plasma membrane, followed by

that in the PVM. Cholesterol from the erythrocyte membrane is acquired by the parasite [13, 14]. The parasite plasma membrane (PPM), which is closely apposed to the PVM has very low amount of cholesterol, making the PPM relatively resistant to cholesterol-dependent detergents such as saponin. The process through which cholesterol gradient is maintained in the infected erythrocytes is not well understood. Although there appears to be little cholesterol inside the trophozoite stage of the parasite, previous studies have shown that erythrocytes with reduced cholesterol content are unable to support *P. falciparum* growth [15].

Recent studies have identified inhibitors of two parasite plasma membrane (PPM) transporters, PfATP4 and PfNCR1, that disrupt cholesterol and lipid homeostasis in the PPM [16, 17]. Upon treatment with these inhibitors, there is a rapid accumulation of cholesterol in the PPM rendering the parasites sensitive to the cholesterol dependent detergent saponin. This was observed as the loss of cytoplasmic protein in drug treated parasites exposed to saponin. This effect was reversible indicating an active mechanism of cholesterol dynamics within the parasite [16]. These unexpected consequences of exposure to novel antimalarials suggest the presence of mechanisms that influence cholesterol transport within intraerythrocytic *P. falciparum*. In this report, we investigate the effects of altering cholesterol content in the erythrocyte plasma membrane on *P. falciparum* development. By using live video microscopy, we show that the removal of cholesterol from the erythrocyte plasma membrane results in dramatic expulsion of trophozoite stage parasites. This process is inhibited by PfATP4 or PfNCR1 inhibitors but not by other antimalarials. The expulsion of parasite was not dependent on the actin polymerization. These studies indicate the critical role played by cholesterol dynamics in the intra erythrocytic development of the parasite

Results:

Cholesterol in the erythrocyte plasma membrane is essential for the development of P. falciparum

To investigate the role of free cholesterol in the erythrocyte membrane on the growth and maturation of *P. falciparum*, we took advantage of cholesterol modulating agent Methyl-β-cyclodextrin (MBCD) (structure in Fig 1A). It has been used extensively to modify membrane cholesterol. Two molecules of MBCD come together to form an 8Å hydrophobic cavity that accommodates a single cholesterol molecule and sterols that are similar in size to cholesterol. MBCD when incubated with cholesterol rich membranes can extract cholesterol and can also donate sterols to deficient membranes [18]. Of note, MBCD can only access the cholesterol in the erythrocyte plasma membrane. We treated the ring stage infected erythrocytes with MBCD for 30 mins. As shown in Fig. 1B, parasites failed to develop in the MBCD treated erythrocytes. Ring stage parasites developed to form trophozoites that had stunted growth and were unable to form mature merozoites capable of undergoing invasion. To investigate if this process is dependent on the amount of cholesterol in the erythrocyte membrane, we performed a complementation assay with various sterols. MBCD-treated, cholesterol deficient erythrocytes were reconstituted with cholesterol, desmosterol or epicholesterol by treating with sterol saturated MBCD (CD/Cho, Cd/Des, CD/Epi) (Fig. 1A). We observed that the ring stage parasites in cholesterol and desmosterol reconstituted cells were able to mature and form schizonts. However, epicholesterol reconstituted ring stage parasites failed to do so. (Fig. 1B). To assess progression of ring stage parasites, we performed a 24 hour hypoxanthine incorporation assay. As shown in Fig 1C, there was significant reduction in hypoxanthine incorporation in MBCD treated and epicholesterol reconstituted parasites, whereas ring stage parasites in cholesterol or desmosterol reconstituted cells were able to incorporate hypoxanthine. These results are consistent with what was observed by examining the Giemsa

115 stained thin blood smears. To assess the viability of these deficient and sterol reconstituted ring
116 stage parasites, we split the culture 1:10 into normal erythrocytes. This was followed by
117 measuring parasitemia over a subsequent four day period. As shown in Fig 1D, ring stage
118 parasites growing in cholesterol depleted or epicholesterol reconstituted cells failed to
119 propagate over the next two cycles. On the other hand, cholesterol or desmosterol reconstituted
120 ring stage parasites were able to propagate at a level of about 50% compared to the control ring
121 stage parasites. These results indicated that cholesterol in the erythrocyte membrane is essential
122 for the parasites to form mature parasites capable of establishing an infection.
123
124 ***Cholesterol in the erythrocyte plasma membrane is essential for P. falciparum invasion***
125 Parasite invasion is a complex process that requires multiple interactions between merozoite
126 surface proteins and receptors on the erythrocyte membrane [19]. We explored the role
127 cholesterol might play in this process by reducing erythrocyte membrane cholesterol. MBCD
128 treated erythrocyte were added to Percoll enriched schizonts. As shown in Fig 2A, removal of
129 cholesterol from uninfected erythrocytes prevented invasion by merozoites. The merozoites
130 remained attached to the surface of MBCD treated erythrocytes but failed to penetrate the cell.
131 As shown in Fig 2B, reconstitution of cholesterol deficient cells with cholesterol,
132 complemented these invasion defects. Furthermore, the parasites were able to grow in these
133 reconstituted erythrocytes and undergo next cycle of growth. Addition of normal erythrocytes
134 to cholesterol deficient or reconstituted cells showed that only parasites from reconstituted cells
135 were able to undergo intraerythrocytic development (Fig. 2C). These results suggest that the
136 cholesterol in the erythrocyte membrane is essential for parasite invasion, and are consistent
137 with previous observations [11, 15].
138 Different *P. falciparum* strains invade using different pathways: a sialic acid dependent or a
139 sialic acid independent pathway [20, 21]. To see if cholesterol in the erythrocyte membrane is

selective for a given pathway, we added either schizonts of NF54 (sialic acid dependent) or Dd2 (sialic acid independent) strains to MBCD treated erythrocytes. Merozoites from neither strain were able to invade MBCD treated erythrocytes (Fig. 2D).

Depletion of cholesterol from erythrocyte plasma membrane causes extrusion of trophozoite stage P. falciparum

A previous study suggested that treatment of trophozoite stage parasites with MBCD releases the parasites from the erythrocyte [22]. We have explored this phenomenon in some detail by using live fluorescent video microscopy. We generated parasites bearing mNeonGreen or mRuby3 fusions to endogenous the C-termini of the PPM protein PfVP1 or PVM protein EXP2. The EXP2-mRuby3 parasites were also engineered with a C-terminal mNeonGreen fusion to RhopH2, which is a rhoptry protein synthesized during late trophozoite stage of the parasite and translocated to the erythrocyte plasma membrane in the ring stage parasite. The use of these parasite lines permitted us monitor the PPM, PVM and internal organelle of the parasite when exposed to MBCD. Remarkably, upon treatment of trophozoite stage infected erythrocyte for 30 mins with MBCD parasites were observed to extrude out of the erythrocyte. This extrusion happens without apparent lysis of the erythrocyte membrane. The parasites that extrude out of the intact erythrocytes are enclosed within the PPM (in green, Fig. 3A) as well as the PVM (in red, Fig. 3B). During the 30 min exposure to MBCD the parasites remain within the erythrocytes but at the end of this period they dramatically emerge out in under 10 seconds (Fig. 3C, Supplementary video 1). Depending upon the plane from which the parasite emerges from the erythrocyte, parts of the PVM is observed still tethered to the host cell. Approximately 70% of trophozoite stage parasites extruded upon MBCD treatment. Quantification of this phenomenon is shown in Fig. 3E. In contrast to the trophozoite stages, cholesterol depletion of ring stage parasites did not result in extrusion; as expected, RhopH2

was localized to the erythrocyte plasma membrane in the ring stage parasite, but the parasite remains inside the host cell (Fig. 3D, Supplementary video 3). Rapid extrusion of the trophozoite from infected erythrocytes prompted us to examine the role of actin filaments in this process. For this, we treated trophozoite-infected erythrocytes with the actin polymerization inhibitor, Cytochalasin D (CytD) [23]. Treatment with CytD prior to MBCD treatment did not inhibit MBCD mediated extrusion of the parasites. Treatment with CytD alone did not cause the parasites to extrude out, however, we did observe defects in the PVM of the CytD treated parasites (Fig. 3F, Supplementary video 2). Although CytD did affect the morphology of the PVM, it failed to prevent extrusion of the parasites when exposed to MBCD.

Transmission electron microscopy of MBCD treated parasites

Electron microscopy of trophozoite stage parasites treated with MBCD show results similar to that observed by live fluorescent video microscopy. Unlike the control group, parasites had extruded out of the MBCD-treated erythrocyte without rupturing the erythrocyte membrane. The parasites were still surrounded by the PVM but the PVM was compromised at multiple places (Fig. 4A). Images shown here are representative of multiple electron micrographs. In another set of experiments, we examined the ring stage parasites by electron microscopy at 24 and 48 hours after treatment with MBCD. As expected at 24 hours the trophozoites in the control group displayed normal morphology with distinctive internal structures and normal hemozoin formation and went on to form ring stages at 48 hours (Fig 4B, top panel). In contrast MBCD treated ring stages showed abnormal morphology with diminished food vacuoles at 24 hours. These parasites failed to develop into normal schizonts and egress at 48 hours after MBCD treatment. (Fig 4B, lower panel). These results are consistent with observations shown in Fig 1B.

Prior Treatment with novel antimalarials abrogates MBCD mediated parasite extrusion

We have previously shown that inhibition of PPM transporters, PfATP4 or PfNCR1 alters cholesterol dynamics in the PPM of trophozoite stage parasites [16, 17, 24]. We therefore wished to examine the effects of these inhibitors on MBCD-mediated extrusion phenomenon. We treated trophozoite stage parasites for 2 hours with KAE609 (a PfATP4 inhibitor) or MMV009108 (a PfNCR1 inhibitor) prior to cholesterol depletion with MBCD. Surprisingly, the parasite extrusion was greatly reduced by prior exposure to both of these inhibitors. Prior treatment with chloroquine, however, did not prevent MBCD mediated extrusion (Fig. 5A). Quantitation of this phenomenon showed that while 80% of parasites extruded in the MBCD and chloroquine treated infected erythrocytes, only about 25% did in the PfATP4 and PfNCR1 inhibitor treated infected erythrocytes (Fig. 5B). This quantitation was also supported by observation of intracellular and extracellular parasites by Giemsa-stained thin blood smear. These results suggest that interference with normal cholesterol dynamics in trophozoite stage parasite is required for MBCD-mediated parasite extrusion phenomenon.

Discussion:

During the intra-erythrocytic development of *P. falciparum*, there is a huge requirement of lipids for the generation of various membranes both within the parasite and inside the host cytoplasm. The erythrocyte plasma membrane contains large amounts of cholesterol (50 mole% of total lipids). Upon infection by Plasmodium, the PVM acquires cholesterol but the PPM remains highly deficient in cholesterol [12, 13]. Indeed, this fact is the basis for widely used saponin mediated freeing of intra-erythrocytic parasites. Our previous observation that disruption of Na+ homeostasis and inhibition of PfNCR1 resulted in accumulation of cholesterol in the PPM [16, 17] prompted us to assess cholesterol dynamics in *P. falciparum*.

For this purpose we used MBCD treatment to reduce cholesterol content within the erythrocyte plasma membrane. Our observation that ring stage parasites growing in cholesterol deficient erythrocytes fail to fully progress could be explained by the inability of the parasite to acquire a subset of essential components from the medium. This could be due to the diminished function of nutrient channels (NPPs) as a result of altered lipid composition of the erythrocyte plasma membrane. Another possibility might be that cholesterol has an active role in importing lipids and/or fatty acids. The fact that cholesterol and desmosterol (but not epicholesterol) could substantially rescue these defects suggest a dynamic interaction of cholesterol and stereospecificity of this interaction underlying the import mechanisms. Additional studies are required to distinguish between these possibilities. Cholesterol deficient erythrocytes also failed to support invasion by merozoites. While extensive investigation will be required to understand the basis of this defect, it is possible that alteration in membrane fluidity or the proper display of receptors may underlie this phenomenon. A recent study using lattice light scattering microscopy demonstrated the importance erythrocyte membrane remodeling for the formation of the PVM, a process in which cholesterol is likely to play a significant role [11].

The dramatic expulsion of the trophozoite stage parasites following MBCD treatment remains unexplained. It is hard to perceive how an intracellular parasite can escape out of the host erythrocyte without causing the lysis of the host membrane in response to reduction in the cholesterol content in the erythrocyte plasma membrane. The force with which the expulsion appears to occur suggest an active process mediated either by the host or the parasite. Our observation that Cytochalasin D did not prevent expulsion of trophozoites indicate that actin polymerization is not required for this process. Osmotic pressure build-up through solute uptake in trophozoites resulting in their release from the host cells has been widely used for synchronization of blood stage *P. falciparum*. However, this requires incubation with high concentrations of solutes such as sorbitol. At 5 mM concentration, MBCD exposure does not

pose an osmotic challenge, and at ~1300 Da molecular weight MBCD would not be taken up by the trophozoite-infected erythrocyte through its new permeability pathway. These observations suggest the possibility of a hitherto unrecognized process through which the parasite might sense cholesterol content of the erythrocyte membrane. MBCD-mediated expulsion of the parasite resembles expulsion of fungal pathogens from the mammalian cells through a process termed vomocytosis wherein the expulsion does not result in lysis of the host cell [25-27]. However, vomocytosis occurs over a period of hours but the expulsion of the trophozoite happens in seconds, suggesting that these two phenomena occur though distinct mechanistic processes.

The dramatic extrusion was inhibited by treatment with compounds inhibiting PfATP4 or PfNCR1. Since we have previously shown that these inhibitors induce cholesterol accumulation in the PPM in a reversible manner it is possible to envision dynamic movement of cholesterol between various membranes of infected erythrocytes. Reduction of the plasma membrane cholesterol content appears to be sensed by the parasite in a manner that results in the expulsion of trophozoites. We suggest that parasite induced cholesterol dynamics plays a major role in the expulsion. Inhibition of these dynamics by PfATP4 or PfNCR1 inhibitors prevents parasite expulsion. This inhibition of expulsion is not a result of mere parasite demise as evidenced by the inability of chloroquine to inhibit expulsion.

In summary, we have uncovered a hitherto unknown role of cholesterol in P. falciparum biology during intra-erythrocytic development. At this point, molecular players participating in this pathway remain unknown but their elucidation may prove to be rewarding.

Methods:

Parasite lines and culture conditions

Experiments were carried out using different P. falciparum tagged lines. 1) 3D7 strain in which endogenous PfVP1 gene was tagged with mNeon green (mNG) at the C-terminal end (PfVP1-mNG). This line was used for monitoring the dynamics of the parasite plasma membrane 2) NF54 strain in which endogenous RhopH2 gene was tagged with mNG and the endogenous Exp2 gene tagged with mRuby3 (NF54 Rhoph2/Exp2). Cloning was carried out with Infusion (Clontech) and NEBuilder HiFi (NEB). To generate an endogenous EXP2-mRuby3 fusion, 5' and 3' homology flanks targeting the 3' end of *exp2* were PCR amplified from plasmid pyPM2GT-EXP2-mNG [28] using primers CACTATAGAACTCGAGGGAGAAACAATCTTTTATATAAAATGTACAGAGTTTGAAAG and TCCTCCACTTCCCCTAGGTTCTTTATTTTCATCTTTTTTTTCATTTTTAAATAAATCTCCAC and inserted between *XhoI* and *AvrII* in the plasmid pbPM2GT [29]. The mRuby3 coding sequence was then amplified from plasmid pLN-HSP101-SP-mRuby3[30] using primers GATGAAAATAAAGAACCTAGGGGAAGTGGAGGAGTG and TAACTCGACGCGGCCGTCACTTGTACAGCTCGTCCATGCC and inserted between *XhoI* and *AvrII*, resulting in the plasmid pbEXP2-mRuby3. This plasmid was linearized at the *AflII* site between the 3′ and 5′ homology flanks and co-transfected with pUF-Cas9-EXP2-CT-gRNA into NF54^{attB}::HSP101^{DDD} [30] . Parasites were maintained in 10 µM trimethoprim to stabilize the HSP101^{DDD} fusion and selection with 2.5 µg/ml Blasticidin S was applied 24 hours post transfection. A clonal line bearing the EXP2-mRuby3 fusion was derived by limiting dilution after parasite returned from selection and designated NF54^{attB}::HSP101^{DDD}+EXP2-mRuby3.

For generation of an endogenous RhopH2-mNG fusion, a gRNA target site was chosen upstream of the *rhoph2* stop codon (TCTTCACTGATTTCTTTGTA) and the gRNA seed sequence was synthesized as a sense and anti-sense primer pair (sense shown)

290 TAAGTATATAATATTTCTTCACTGATTTCTTTGTAGTTTTAGAGCTAGAA, annealed
291 and inserted into the *AflII* site of the plasmid pAIO3 [31], resulting in the plasmid pAIO3-
292 RhopH2-CT-gRNA. To integrate mNG at the 3' end of *rhoph2*, a 5' homology flank (up to
293 but not including the stop codon) was amplified from NF54^{attB} genomic DNA using primers
294 AATTTCATCATTATGAAAGTTCTCAGCTTAAGAAGCATATATTAAGAATATAGTT
295 TCAGA and
296 CCTCCACTTCCCCTAGGACTGCTCTTCAGAATATACAGGTTTTTTATAAGATCCTC
297 CGATATCTCCTTATATGGATCAGATATATCTGAGAAA, incorporating several
298 synonymous mutations in the seed sequence of the gRNA target site within the *rhoph2*
299 coding sequence. A 3' homology flank (beginning at the endogenous stop codon) was
300 amplified using primers
301 GTGACACTATAGAACTCGAGTAAACGTTAAAAAAAAAATATATATAAGGAGAAA
302 GCACTG and
303 TCTGAAACTATATTCTTAATATATGCTTCTTAAGCTGAGAACTTTCATAATGATGA
304 AATT, assembled in a second PCR reaction using primers
305 GTGACACTATAGAACTCGAGTAAACGTTAAAAAAAAAATATATATAAGGAGAAA
306 GCACTG and
307 CCTCCACTTCCCCTAGGACTGCTCTTCAGAATATACAGGTTTTTTATAAGATCCTC
308 CGATATCTCCTTATATGGATCAGATATATCTGAGAAA and inserted between *XhoI*
309 and *AvrII* in pyPM2GT-EXP2-mNG [28] resulting in the plasmid pyPM2GT-RhopH2-mNG.
310 This plasmid was linearized at the *AflII* site between the 3' and 5' homology flanks and co-
311 transfected with pAIO3-RhopH2-CT-gRNA into NF54^{attB}::HSP101^{DDD}+EXP2-mRuby3.
312 Selection with 2 µM DSM-1 was applied 24 hours post transfection (along with 10 µM
313 trimethoprim). After parasites returned from selection, a clonal line containing the EXP2-
314 mRuby3 and RhopH2-mNG fusions was obtained by limiting dilution and designated

315 NF54^{attB}::HSP101^{DDD}+EXP2-mRuby3+RhopH2-mNG. This line was used for monitoring the
316 parasitophorous vacuolar membrane and to mark the parasite. *P. falciparum* parasites were
317 cultured in O^+ human blood from Interstate Blood Bank, TN in RPMI 1640 supplemented
318 with 2g/L sodium bicarbonate, 10mg/L hypoxanthine, 15mM HEPES, 50mg/L gentamycin
319 sulphate, 0.5% AlbuMax II. Parasite culture was maintained at 2.5% hematocrit at 37 °C in
320 90% N_2, 5% CO_2, 5% O_2.

321

322 **Preparation of MBCD and MBCD-sterol complexes**

323 Parasites were treated with 5mM MBCD diluted in appropriate medium from a stock solution
324 of 25mM MBCD (Catalog no. AC377110250) in PBS in appropriate medium. Sterols
325 [Cholesterol (Sigma, C3045-25G) , Desmosterol (Steraloids, catalog no. C3150-000),
326 Epicholesterol (Steraloids, catalog no. C6730-000)] were loaded onto MBCD according to
327 previously published protocol [32]. Briefly, 10µL of 15mg/ml sterols dissolved in ethanol were
328 added to 500µL 5% w/v MBCD, heated for 10 mins at 80°C and mixed by inverting several
329 times until the solution was clear. The above step was repeated 4 times to add a total of 50µL
330 sterol stock solution. The solution was heated until the sterols were stably incorporated in
331 MBCD (clear solution). MBCD/sterol complexes were snap frozen in dry ice for 2 mins.
332 Subsequently, the MBCD/sterol complexes were lyophilized in a speed vac until all liquid had
333 evaporated and a fluffy powered remained at the bottom of the tube and stored at -20°C.
334 Immediately before use, 375µl of medium was added to the MBCD/sterol complexes and
335 vortexed until dissolved. The MBCD/sterol complexes were sterilized using 0.22µm syringe
336 filter.

337

338 **Treatment of parasitized erythrocytes with MBCD and reconstitution with MBCD/sterol**
339 **complexes**

Parasite cultures were synchronized by treatment with 0.5mM alanine for 10 minutes. Erythrocyte infected with ring stage parasites were treated with 5mM MBCD for 30 mins at 37C and washed 3 times with pre-warmed RPMI1640 media. Hematocrit was maintained at 2.5% throughout the culture and washing steps. The parasites were returned to normal culture conditions. In experiments involving reconstitution with MBCD/sterol complexes, parasites were first treated with MBCD as discussed above. Following this, the cells were incubated with 1:7 dilution of MBCD/sterol complexes for 30 mins. Parasites were washed 3 times and returned to normal culture conditions. Giemsa stained thin blood smears were prepared 24 and 48 hours after the treatment with MBCD or after reconstitution with MBCD/sterol complexes. The culture at 48 hours was split 1:10 in normal erythrocytes. Growth of the parasites in these cultures were followed for 4 days by examining Giemsa stained thin blood smears

Hypoxanthine incorporation of ring stage erythrocyte treated with MBCD or MBCD/sterol complexes

Ring stage erythrocyte (1.5% parasitemia) were treated with MBCD for 30 mins and washed 3 times with normal medium. The hematocrit was maintained at 2.5%. MBCD-treated ring stage erythrocytes were then treated with either MBCD/cholesterol, MBCD/desmosterol or MBCD/epicholesterol for 30 mins and washed 3 times with low hypoxanthine medium. The hematocrit was then adjusted to 1.5% by addition of low hypoxanthine medium to the cells. 200µl of cells were then plated in triplicates in a 96-well plate. Each well was pulsed with 22µl of 0.5 µCi/ml ^{3}H-hypoxanthine (PerkinElmer NET 177) and incubated for 24 hours at 37ºC in 5% CO_2, 5% O_2 chamber. Parasites were lysed by freeze/thaw and were collected on filters using a cell harvester (PerkinElmer LifeSciences). This was followed by addition of MicroScint O scintillation cocktail and incorporation of ^{3}H-hypoxanthine was measured using a TopCount scintillation counter (PerkinElmer Life-sciences).

365

366 **Parasite invasion in MBCD or MBCD/Cholesterol treated erythrocytes**

367 We treated 500µl of 50% hematocrit erythrocytes with 5mM MBCD for 30 mins followed by
368 3 washes. In addition, similarly treated erythrocytes were reconstituted with
369 MBCD/Cholesterol for 30 mins followed by 3 washes. Synchronized late stages trophozoites
370 were enriched by centrifugation over a 70% Percoll cushion (3000 RPM, 20 mins) and washed
371 thrice with medium. Enriched late stage trophozoites were added to MBCD treated ,
372 MBCD/Cholesterol reconstituted and control erythrocytes. Giemsa-stained thin blood smears
373 were prepared 24 and 48 hours following the addition. The culture at 48 hours was split 1:10
374 in normal erythrocytes. Growth of the parasites in these cultures were followed for 4 days by
375 examining Giemsa-stained thin blood smears.

376

377

378 **Live microscopy of parasites**

379 Glass bottom culture dishes (35 mm) were coated with 0.1% poly-l-lysine overnight and
380 washed 3 times with PBS. Parasite culture (250µl at 2.5% hematocrit) was added to the dishes
381 and incubated for 30 mins to allow attachment. Culture dishes were washed 3 times with PBS
382 followed by addition of medium. For MBCD extrusion experiments with NF54 Rhoph2/Exp2,
383 all washes, incubation and imaging was done in medium supplemented with TMP. Parasites
384 were attached to poly-l-lysine coated plates and incubated in RPMI containing wheat germ
385 agglutinin-Alexa 350 (WGA-350) (Invitrogen, Catalog no. W7024) at 5µg/ml final
386 concentration and incubated for 12 mins to stain the erythrocyte plasma membrane. In addition
387 to WGA staining, PfVP1-mNG line was also stained with SYTO deep red nuclear stain for 30
388 min. Parasites were treated with 5mM MBCD followed by three washes with medium. The
389 medium was replaced with phenol red free medium followed by live fluorescent microscopy.

Imaging was done using the Nikon Ti microscope. WGA-Alexa-350 was visualized using DAPI filter set, mNeon green with FITC, SYTO deep red nuclear stain with Cy5 and mRuby was visualized using TRITC filter set.

Inhibition of MBCD mediated extrusion by novel antimalarials.

To look at the effects of antimalarials on MBCD mediated extrusion, parasites were stained with WGA-350 and SYTO deep red for PfVP-1mNG line or WGA-350 for NF54 Rhoph2/Exp2 line as described above and treated with 10XEC_{50} concentrations of Choloroquine (150nM), KAE609 (10nM) and MMV009108(1µM) for 2.5 hours prior to 30 mins treatment with MBCD and washed thrice with medium. Medium supplemented with drugs (at the concentration mentioned above) was added back to the dish and live fluorescent imaging was carried out. Quantification of parasites remaining inside/outside of erythrocytes was carried out by examining at least 100 different images of individual parasites for each experimental condition.

Cytochalasin D (Cyt-D) treatment prior to MBCD treatment of parasites

Attached NF54 RhopH2/Exp2 trophozoites were stained with WGA-350 for 12 mins, followed by three washes. The cells were then treated with 0.5µM Cyt-D for 45 mins. This was followed by the addition of 5mM MBCD for 30 mins. The culture dishes were washed 3 times and live fluorescent microscopy was performed to examine parasite extrusion. In the control condition, parasites were treated with Cyt-D without MBCD treatment.

Transmission electron microscopy of trophozoite infected MBCD treated erythrocytes

Erythrocytes infected with trophozoite stage parasites were treated with 5mM MBCD for 30 mins at 2.5% hematocrit followed by three washes with PBS and incubated in complete

415 medium for 30 mins at 37 °C. Cells were washed once in PBS by gentle centrifugation and
416 fixed with 2% paraformaldehyde, 2.5% glutaraldehyde in 100 mM cacodylate buffer and were
417 fixed for 1 hour at room temperature. Cells were gently pelleted by centrifugation, resuspended
418 in cacodylate buffer and immediately stored on dry ice for shipment.
419 Ring stage infected erythrocytes were treated with 5mM MBCD for 30 mins, washed thrice
420 with PBS and returned to culture at 37 °C. At 24 and 48 hours subsequent to the treatment,
421 infected erythrocytes were fixed and prepared for transmission electron microscopy as
422 described above.
423

424 **Acknowledgements:**
425 We thank the members of Vaidya lab for lively discussion and input. This work was
426 supported by a National Institutes of Health grant R01 AI132508 to ABV and R00 HL133453
427 to JRB.

References:

1. *World malaria report 2020, WHO*. 2020.
2. Cassera, M.B., et al., *The methylerythritol phosphate pathway is functionally active in all intraerythrocytic stages of Plasmodium falciparum.* J Biol Chem, 2004. **279**(50): p. 51749-59.
3. Gerold, P. and R.T. Schwarz, *Biosynthesis of glycosphingolipids de-novo by the human malaria parasite Plasmodium falciparum.* Mol Biochem Parasitol, 2001. **112**(1): p. 29-37.
4. Maguire, P.A. and I.W. Sherman, *Phospholipid composition, cholesterol content and cholesterol exchange in Plasmodium falciparum-infected red cells.* Mol Biochem Parasitol, 1990. **38**(1): p. 105-12.
5. Vial, H.J., et al., *Biosynthesis and dynamics of lipids in Plasmodium-infected mature mammalian erythrocytes.* Blood Cells, 1990. **16**(2-3): p. 531-55; discussion 556-61.
6. Vial, H.J., J.R. Philippot, and D.F. Wallach, *A reevaluation of the status of cholesterol in erythrocytes infected by Plasmodium knowlesi and P. falciparum.* Mol Biochem Parasitol, 1984. **13**(1): p. 53-65.
7. Holz, G.G., Jr., *Lipids and the malarial parasite.* Bull World Health Organ, 1977. **55**(2-3): p. 237-48.
8. Labaied, M., et al., *Plasmodium salvages cholesterol internalized by LDL and synthesized de novo in the liver.* Cell Microbiol, 2011. **13**(4): p. 569-86.
9. Grellier, P., et al., *Lipid traffic between high density lipoproteins and Plasmodium falciparum-infected red blood cells.* J Cell Biol, 1991. **112**(2): p. 267-77.
10. Coppens, I. and O. Vielemeyer, *Insights into unique physiological features of neutral lipids in Apicomplexa: from storage to potential mediation in parasite metabolic activities.* Int J Parasitol, 2005. **35**(6): p. 597-615.
11. Geoghegan, N.D., et al., *4D analysis of malaria parasite invasion offers insights into erythrocyte membrane remodeling and parasitophorous vacuole formation.* Nat Commun, 2021. **12**(1): p. 3620.
12. Tokumasu, F., et al., *Inward cholesterol gradient of the membrane system in P. falciparum-infected erythrocytes involves a dilution effect from parasite-produced lipids.* Biol Open, 2014. **3**(6): p. 529-41.
13. Hayakawa, E.H., et al., *Real-time cholesterol sorting in Plasmodium falciparum-erythrocytes as revealed by 3D label-free imaging.* Sci Rep, 2020. **10**(1): p. 2794.
14. Fraser, M., et al., *Breakdown in membrane asymmetry regulation leads to monocyte recognition of P. falciparum-infected red blood cells.* PLoS Pathog, 2021. **17**(2): p. e1009259.
15. Samuel, B.U., et al., *The role of cholesterol and glycosylphosphatidylinositol-anchored proteins of erythrocyte rafts in regulating raft protein content and malarial infection.* J Biol Chem, 2001. **276**(31): p. 29319-29.
16. Das, S., et al., *Na+ Influx Induced by New Antimalarials Causes Rapid Alterations in the Cholesterol Content and Morphology of Plasmodium falciparum.* PLoS Pathog, 2016. **12**(5): p. e1005647.
17. Istvan, E.S., et al., *Plasmodium Niemann-Pick type C1-related protein is a druggable target required for parasite membrane homeostasis.* Elife, 2019. **8**.
18. Mahammad, S. and I. Parmryd, *Cholesterol depletion using methyl-β-cyclodextrin.* Methods Mol Biol, 2015. **1232**: p. 91-102.
19. Sisquella, X., et al., *Plasmodium falciparum ligand binding to erythrocytes induce alterations in deformability essential for invasion.* eLife, 2017. **6**: p. e21083.

20. Camus, D. and T.J. Hadley, *A Plasmodium falciparum antigen that binds to host erythrocytes and merozoites.* Science, 1985. **230**(4725): p. 553-6.
21. Dolan, S.A., L.H. Miller, and T.E. Wellems, *Evidence for a switching mechanism in the invasion of erythrocytes by Plasmodium falciparum.* J Clin Invest, 1990. **86**(2): p. 618-24.
22. Lauer, S., et al., *Vacuolar uptake of host components, and a role for cholesterol and sphingomyelin in malarial infection.* The EMBO journal, 2000. **19**(14): p. 3556-3564.
23. Casella, J.F., M.D. Flanagan, and S. Lin, *Cytochalasin D inhibits actin polymerization and induces depolymerization of actin filaments formed during platelet shape change.* Nature, 1981. **293**(5830): p. 302-5.
24. Bhatnagar, S., et al., *Diverse Chemical Compounds Target Plasmodium falciparum Plasma Membrane Lipid Homeostasis.* ACS infectious diseases, 2019. **5**(4): p. 550-558.
25. Cruz-Acuña, M., N. Pacifici, and J.S. Lewis, *Vomocytosis: Too Much Booze, Base, or Calcium?* mBio, 2019. **10**(6).
26. Nicola, A.M., et al., *Nonlytic exocytosis of Cryptococcus neoformans from macrophages occurs in vivo and is influenced by phagosomal pH.* mBio, 2011. **2**(4).
27. Seoane, P.I. and R.C. May, *Vomocytosis: What we know so far.* Cell Microbiol, 2020. **22**(2): p. e13145.
28. Glushakova, S., et al., *Exploitation of a newly-identified entry pathway into the malaria parasite-infected erythrocyte to inhibit parasite egress.* Sci Rep, 2017. **7**(1): p. 12250.
29. Beck, J.R., et al., *PTEX component HSP101 mediates export of diverse malaria effectors into host erythrocytes.* Nature, 2014. **511**(7511): p. 592-5.
30. Glushakova, S., et al., *Rounding precedes rupture and breakdown of vacuolar membranes minutes before malaria parasite egress from erythrocytes.* Cell Microbiol, 2018. **20**(10): p. e12868.
31. Nessel, T., et al., *EXP1 is required for organisation of EXP2 in the intraerythrocytic malaria parasite vacuole.* Cell Microbiol, 2020. **22**(5): p. e13168.
32. Luu, W., I.C. Gelissen, and A.J. Brown, *Manipulating Cholesterol Status Within Cells.* Methods Mol Biol, 2017. **1583**: p. 41-52.

509

510 **Figure Legends**

511

512 **Figure 1:** Cholesterol in the erythrocyte membrane is essential for growth and proliferation of
513 *P. falciparum*.

514 (A) Structure of MBCD, Cholesterol, Epicholesterol and Desmosterol. The differences
515 between the structure of sterols are highlighted in red. (B) Giemsa-stained thin blood smears
516 prepared from control, MBCD and erythrocytes reconstituted with cholesterol, desmosterol or
517 epicholesterol at 24 and 48 hours after treatment. (C) Relative (^{3}H)-hypoxanthine incorporation
518 by ring stage parasites over a 24 hour period following treatment with MBCD or reconstituted
519 with cholesterol, desmosterol and epicholesterol. Based on unpaired t-test with Welch's
520 correction (* $p<0.05$, *** $p<0.001$). Error bars=mean±SD N=8. (D) Relative parasitemia in
521 1:10 split of ring stage parasites from control, MBCD or erythrocytes reconstituted with
522 cholesterol, desmosterol or epicholesterol over 4 days (~3000 cells were counted). Parasitemia
523 in the control culture was normalized to 100%.

524

525 **Figure 2:** Reducing the cholesterol content in the erythrocyte membrane inhibits *P. falciparum*
526 invasion

527 (A) Giemsa stained thin blood smears from control and MBCD treated erythrocytes after 24
528 hours. While ring stages were seen in the control erythrocytes, no invasion was seen in the
529 MBCD treated erythrocytes but merozoites appeared to remain attached to the surface as
530 indicated by arrows. (B) Percoll enriched trophozoites were added to erythrocytes treated with
531 MBCD or reconstituted with cholesterol and giemsa stained thin blood smears were prepared
532 at 24 and 48 hours. Reconstituted erythrocytes were able to support parasite growth. (C)
533 Relative parasitemia from 1:10 spilt of culture from MBCD treated and reconstituted with
534 cholesterol in normal erythrocytes over a period of 4 days (~1000 cells were counted). (D)

535 Percoll synchronized trophozoites from NF54 and Dd2 strains were added onto MBCD treated
536 erythrocytes. Relative parasitemia from 1:10 split of these cultures by examining Giemsa
537 stained thin blood smears (~1000 cells were counted). Parasitemia in the control culture were
538 normalized to 100%.
539
540 **Figure 3:** Trophozoites extrude out from erythrocyte upon treatment with MBCD.
541 (A) Representative images (>50) of PfVP1- mNG line after MBCD treatment. Nucleus is
542 stained with SYTO-deep red (Pink). (B) Representative images (>50) of NF54 RhopH2/Exp2
543 line after MBCD treatment. Erythrocyte membrane is stained with WGA-Alexa-350 (Blue).
544 Infected erythrocytes were subjected to live fluorescent microscopy after treatment with
545 MBCD. Parasites extrude out from erythrocyte without causing lysis of the erythrocyte with
546 their PPM (A) and PVM (B) still attached to the erythrocyte as indicated by the arrows. (C)
547 Still frames from Supplementary video 1 from time lapse video microscopy performed at 30
548 sec intervals for 10 mins. Parasites extrude out from the erythrocyte with the PVM still tethered
549 to the erythrocyte membrane without causing the lysis of erythrocyte (indicated by arrows).
550 (D) Representative images of erythrocytes infected with ring stages of the NF54 RhopH2/Exp2
551 line treated with MBCD. Ring stage parasites do not extrude out from erythrocytes. (E)
552 Quantification of parasites remaining inside/outside of erythrocytes after MBCD treatment was
553 carried out by examining at least 100 different images of individual parasites for each
554 experimental condition (100 for ring stages and 330 for trophozoites). (F) Upper panel:
555 Treatment of NF54 RhopH2/Exp2 trophozoites with 0.5 µM Cyt-D for 45 mins prior to MBCD
556 treatment does not inhibit parasite extrusion. Lower panel: Treatment with 0.5 µM Cyt-D alone
557 does not cause extrusion of trophozoites but did alter PVM morphology (as indicated by
558 arrows)
559

560 **Figure 4:** Transmission electron microscopy of the parasites treated with MBCD: (A)
561 (Left)Treatment with MBCD causes extrusion of *P. falciparum* stage trophozoites without
562 causing erythrocyte rupture unlike the control group where the trophozoite is still inside the
563 erythrocyte. (Right) Zoomed in image of parasite extruded out of erythrocyte after MBCD
564 treatment shows the PVM ruptured at multiple places indicated by black arrows. (B) TEM of
565 the ring stage erythrocyte treated with 5mM MBCD and imaged after 24 or 48 hours.
566 (Left)After 24 hours, in erythrocyte treated with MBCD, parasites are unable to form normal
567 trophozoites. The nuclear membrane is indistinct, hemozoin is dispersed (indicated by arrows)
568 and food vacuole is small compared to control erythrocytes. (Right) After 48 hours, parasites
569 in the control culture were able to invade the erythrocyte and form rings while the parasites in
570 the MBCD treated erythrocytes undergo did not progress further and appear to disintegrate.
571
572 **Figure 5:** Treatment with PfATP4 or PfNCR1 inhibitors prior to MBCD treatment inhibited
573 MBCD mediated extrusion of parasites: (A) Trophozoite stage parasites from PfVP1-mNG
574 line were treated with KAE609 (10nM), MMV009108 (1μM) and chloroquine (150nM) prior
575 to treatment with MBCD. Live fluorescent imaging showed that parasite extrusion was
576 inhibited by prior treatment with KAE609 and MMV009108 (indicated by yellow arrows)
577 while treatment with chloroquine like MBCD did not inhibit this extrusion (indicated by white
578 arrows). Nucleus is stained with SYTO-deep red (pink). Erythrocyte membrane is stained with
579 WGA-Alexa-350 (Blue). Representative images from 3 independent experiments for each
580 condition (B) Quantification from live fluorescent microscopy experiments of parasite
581 extrusion upon drug treatment followed by MBCD treatment. Approximately 250 cells for each
582 experimental condition over 4 independent experiment were assessed.
583

584 **Supplementary Videos**

585 **Supplementary video 1:** Treatment with MBCD causes extrusion of trophozoites from
586 erythrocytes
587 Representative time lapse video microscopy of the NF54 RhopH2/Exp2 line after MBCD
588 treatment. Erythrocyte membrane is stained with WGA-Alexa-350 (Blue). Infected
589 erythrocytes were subjected to live fluorescent microscopy after treatment with MBCD.
590 Parasites extrude out from erythrocyte without causing lysis of the erythrocyte. Video was
591 acquired using the Nikon Ti microscope. Microscopy was performed by taking images at 30
592 seconds interval for 10 mins . Images were deconvoluted by Richardson Lucy algorithm
593 using the Nikon NIS elements software package and converted to .avi files.
594
595 **Supplementary video 2:** Cyt-D treatment does not inhibit MBCD mediated parasite
596 extrusion
597 Representative time lapse video microscopy of the NF54 RhopH2/Exp2 line after MBCD
598 treatment. Erythrocyte membrane is stained with WGA-Alexa-350 (Blue). Infected
599 erythrocytes were subjected to live fluorescent microscopy after treatment with Cyt-D
600 followed by treatment with MBCD. Treatment with Cyt-D does not inhibit MBCD mediated
601 extrusion of the parasite. Video microscopy was performed as mentioned above for video 1.
602
603 **Supplementary movie 3:** Treatment with MBCD does not cause extrusion of ring stage
604 parasites
605 Erythrocytes infected with ring stages of the NF54 RhopH2/Exp2 were treated with MBCD .
606 Erythrocyte membrane is stained with WGA-Alexa-350 (Blue). Ring stage parasites do not
607 extrude out after MBCD treatment. Video microscopy was performed as mentioned for video
608 1.

FIGURE 1:

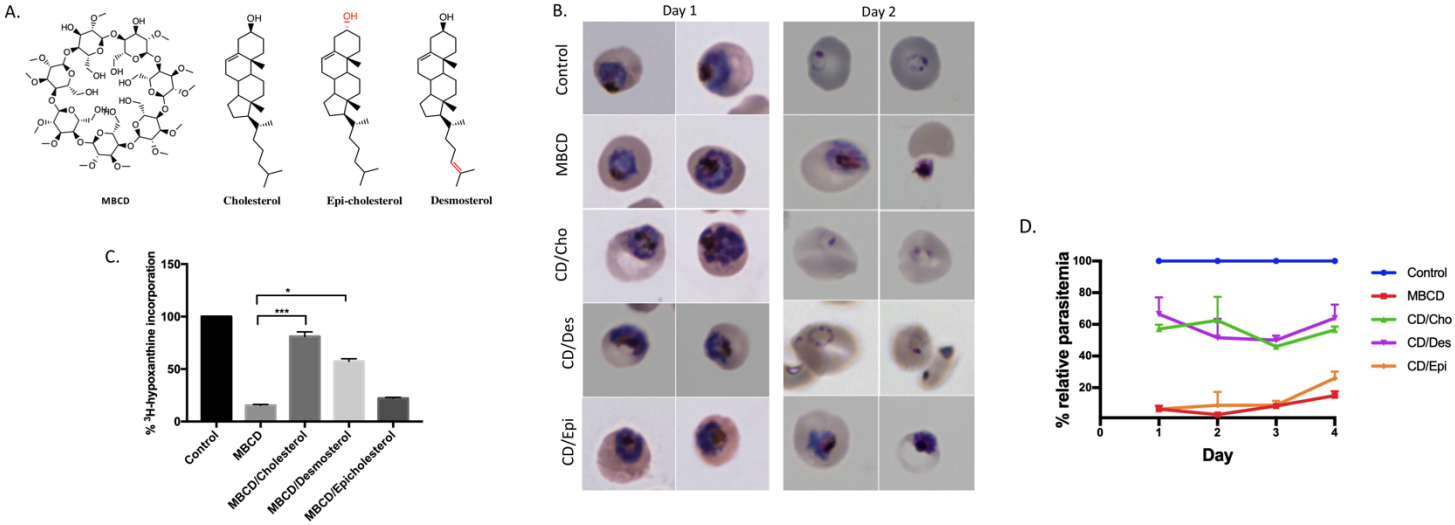

FIGURE 2:

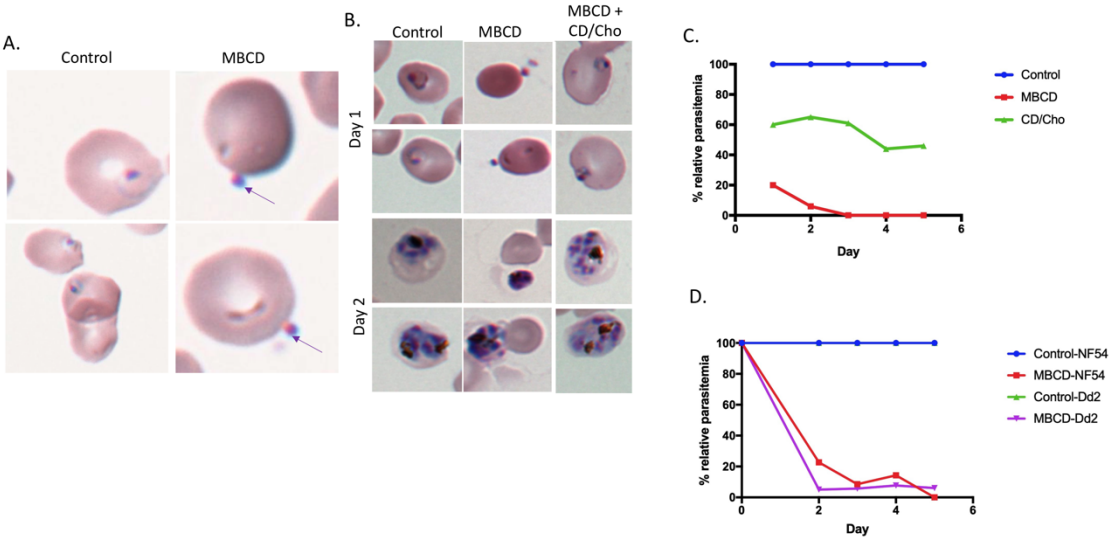

FIGURE 3:

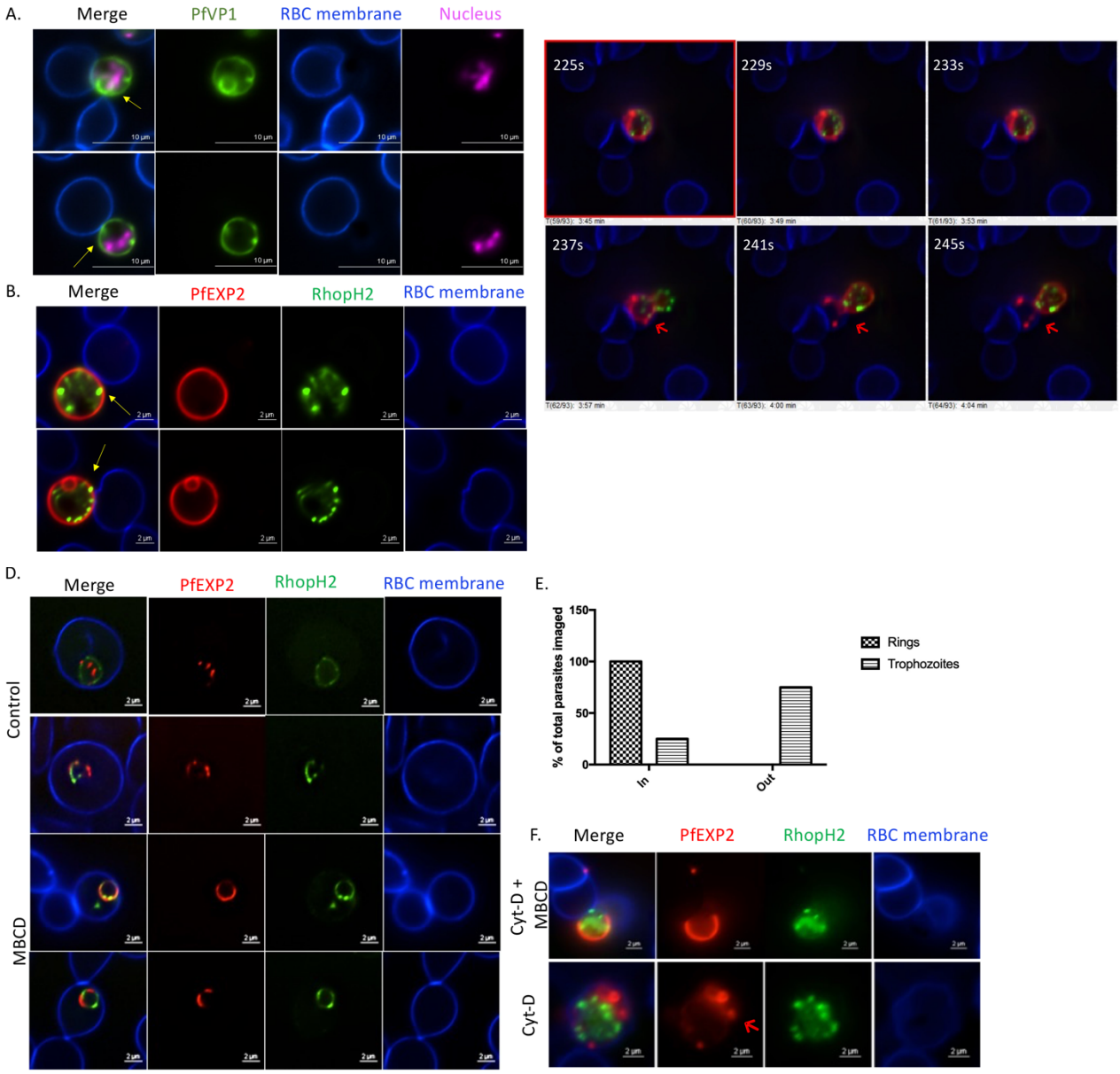

FIGURE 4:

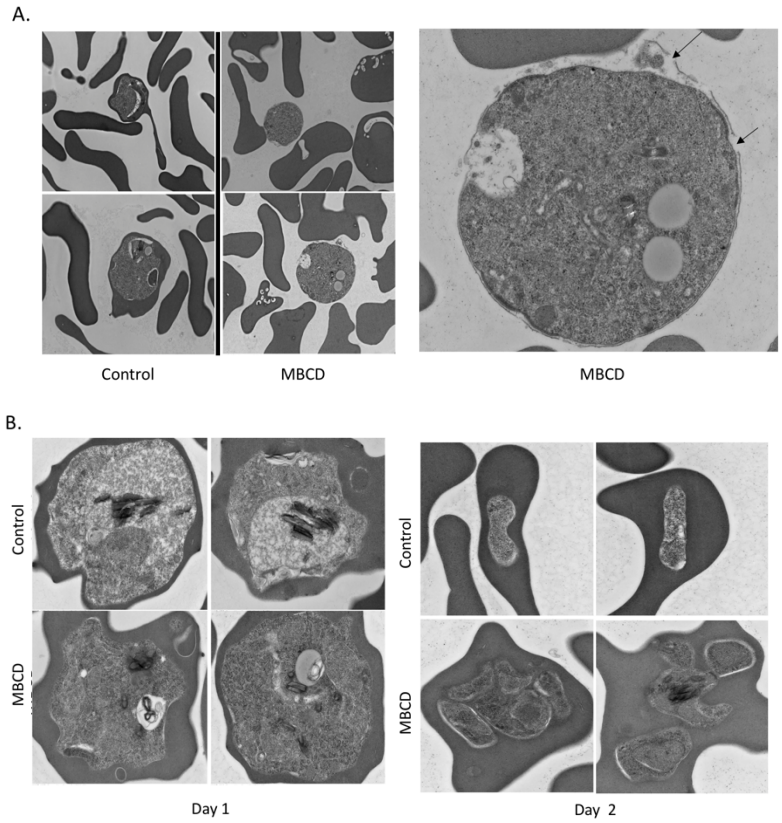

FIGURE 5: